

## Supporting information

# Electrostatically Driven Lipid-Lysozyme Mixed Fibers Display a Multilamellar Structure without Amyloid Features

Ana M. Melo<sup>a</sup>, Luís M.S. Loura<sup>b,c</sup>, Fábio Fernandes<sup>a</sup>, José Villalaín<sup>d</sup>, Manuel Prieto<sup>a</sup>,  
and Ana Coutinho<sup>\*,a,e</sup>

<sup>a</sup> Centro de Química-Física Molecular and Institute of Nanoscience and Nanotechnology, Instituto Superior Técnico, Universidade de Lisboa, Av. Rovisco Pais, 1049-001 Lisboa, Portugal

<sup>b</sup> Faculdade de Farmácia, Universidade de Coimbra, 3000-548 Coimbra, Portugal

<sup>c</sup> Centro de Química de Coimbra, 3004-535 Coimbra, Portugal

<sup>d</sup> Instituto de Biología Molecular y Celular, Universidad Miguel Hernández, E-03202 Elche-Alicante, Spain

<sup>e</sup> Dep. Química e Bioquímica, Faculdade de Ciências, Universidade de Lisboa, Campo Grande, 1749-016 Lisboa, Portugal

\* To whom correspondence should be addressed. E-mail: [ana.coutinho@ist.utl.pt](mailto:ana.coutinho@ist.utl.pt)

## Table of Contents

### Experimental Procedures and Data Analysis

Laurdan generalized polarization measurements .....	S3
Fluorescence recovery after photobleaching (FRAP) measurements.....	S3
Fluorescence intensity decay analysis .....	S5
FRET data analysis.....	S5
Infrared spectroscopy .....	S8

### Supporting Figures and Table

Figure S1 .....	S9
Figure S2 .....	S10
Figure S3 .....	S11
Table S1 .....	S12

<b>References .....</b>	<b>S13</b>
-------------------------	------------

### **Laurdan generalized polarization measurements**

The  $G$ -factor was calculated by acquiring images of Laurdan in dimethyl sulfoxide (DMSO) using the same microscope settings as in the GUV/mixed fiber measurements and considering the following equation:

$$G = \frac{I_{(400-460)}(1 - GP_{\text{bulk}}^{\text{ref}})}{I_{(470-530)}(1 + GP_{\text{bulk}}^{\text{ref}})} \quad (\text{S1})$$

where  $GP_{\text{bulk}}^{\text{ref}}$  is the generalized polarization value from the reference solution measured in a SLM-AMINCO 8100 spectrofluorometer (SLM Instruments Inc., Urbana, IL) using one-photon excitation (1PE) at 350 nm. The  $GP_{\text{bulk}}^{\text{ref}}$  obtained for Laurdan in DMSO was 0.02. Eqn (1) (with  $G = 1$ ) was also used to calculate  $GP_{\text{bulk}}$  but now  $I_{(400-460)}$  and  $I_{(470-530)}$  represent the integrated fluorescence intensities of the emission spectra of Laurdan at the indicated wavelengths intervals. Pseudo-colored generalized polarization images and histograms were obtained using Matlab (The MathWorks, Inc.) and ImageJ free software. The mean 2PE generalized polarization values,  $GP_{\text{micro}}^{\text{mean}}$ , were obtained by nonlinear fitting one or two Gaussian distributions to the generalized polarization histograms.

### **Fluorescence recovery after photobleaching (FRAP) measurements**

FRAP experiments carried out with GUVs started with the acquisition of 10 image scans at low laser intensity. Then, NBD fluorescence was bleached locally inside the region of interest (ROI), using a scan of 3 frames at high laser intensity. Finally, the fluorescence redistribution was monitored by the acquisition of a series of 150 images with the same low laser intensity as before the bleach. In all steps, the images were

acquired using a frame size of  $256 \times 256$  pixels and a bidirectional scan at a 1400 Hz line frequency scan speed, which gave a time-lapse of 0.113 s. Essentially the same protocol was used for the FRAP measurements performed on the lipid-protein fibers. However, as the lipid and protein diffusion in these structures is much slower, only 2 scans were used to bleach inside the ROI and the postbleach phase was extended by acquiring 75 extra images with a time interval of 0.6 s. The pinhole was set to 222.92  $\mu\text{m}$  (2 Airy) and a zoom of  $6\times$  was employed.

The analysis of raw FRAP data was performed using the FRAP Analyser software version 1.0.5.<sup>1</sup> Specifically, the double normalized fluorescence recovery curves<sup>2</sup> were analyzed considering a model for uniform disk illumination profile:<sup>3</sup>

$$F(t) = F(0) + (F(\infty) - F(0)) \cdot e^{-2\tau_D/t} \left[ I_0 \left( \frac{2\tau_D}{t} \right) + I_1 \left( \frac{2\tau_D}{t} \right) \right] \quad (\text{S2})$$

where  $F(t)$ ,  $F(0)$  and  $F(\infty)$  are the normalized fluorescence intensities at time  $t$ ,  $t = 0$  and  $t \rightarrow \infty$ , respectively.  $\tau_D$  is the characteristic diffusion time, and  $I_0$  and  $I_1$  are modified Bessel functions. The 2D lateral diffusion coefficients were calculated from:

$$\tau_D = \frac{\omega^2}{4D} \quad (\text{S3})$$

Where  $\omega$  is the radius of the disk-shaped bleached ROI ( $\omega = 2.5 \mu\text{m}$ ). The mobile fractions,  $M_f$ , were calculated directly from the FRAP normalized recovery curves as:<sup>1</sup>

$$M_f = (F(\infty) - F(0)) / (F^{\text{pre\_bleach}} - F(0)) \quad (\text{S4})$$

where  $F^{\text{pre\_bleach}}$  is the normalized fluorescence intensity before the bleach.

## Fluorescence intensity decay analysis

Bulk fluorescence decay curves were analyzed using a sum of discrete exponential terms:

$$I(t) = \sum_{i=1}^n a_i \cdot \exp(-t/\tau_i) \quad (\text{S5})$$

where  $a_i$  and  $\tau_i$  are the amplitude and the lifetime of the  $i$ th decay component of fluorescence, respectively. Data analysis was performed using the TRFA Data Processing Package version 1.4 of the Scientific Software Technologies Center (Belarusian State University) and the usual statistical criteria, namely a reduced  $\chi^2$  value  $< 1.3$  and a random distribution of weighted residuals and autocorrelation plots, were used to evaluate the goodness of the fits. The amplitude-weighted mean fluorescence lifetime,  $\langle\tau\rangle_1$ , proportional to the quantum yield, was calculated using eqn (S6), where  $\alpha_i$  are the normalized amplitudes:

$$\langle\tau\rangle_1 = \sum_{i=1}^n \alpha_i \cdot \tau_i \quad (\text{S6})$$

The experimental Förster resonance energy transfer (FRET) efficiency of each sample,  $E_{\text{FRET}}^{\text{bulk}}$ , was obtained using eqn (S7):

$$E_{\text{FRET}}^{\text{bulk}} = 1 - \frac{\langle\tau\rangle_1^{\text{DA}}}{\langle\tau\rangle_1^{\text{D}}} \quad (\text{S7})$$

Here,  $\langle\tau\rangle_1^{\text{D}}$  and  $\langle\tau\rangle_1^{\text{DA}}$  are the amplitude-weighted mean fluorescence lifetimes of the donor in the absence and presence of acceptors, respectively.

## FRET data analysis

In order to gain quantitative topological information about the FRET system under study, time-resolved bulk FRET experiments were further globally analyzed using FRET formalisms derived previously to describe interplanar energy transfer between a

surface-bound fluorescently-labeled protein (D) and a membrane probe acceptor (A) randomly distributed in a lipid bilayer.<sup>4-7</sup> According to the cooperative partition model of Lz-A488 presented earlier,<sup>8</sup> in the presence of 430  $\mu\text{M}$  POPC LUVs prepared with 20 mol% of POPS there is always a significant fraction of free monomeric Lz-A488 in solution,  $x_D^w$ . These free donors are molecules too distant from the membrane-embedded acceptors and therefore cannot undergo Förster energy transfer, artefactually decreasing the experimental FRET efficiency. To take this effect into account, both the time-resolved fluorescence laws used to describe the decays measured for the samples D and DA ( $I_D(t)$  and  $I_{DA}(t)$ , respectively) should allow for a fraction  $x_D^w$  of donor molecules whose fluorescence decay is unaffected by the acceptors:<sup>5</sup>

$$I_D(t) = x_D^w \cdot I_D^w(t) + (1 - x_D^w) \cdot I_D^m(t) \quad (\text{S8})$$

$$I_{DA}(t) = x_D^w \cdot I_D^w(t) + (1 - x_D^w) \cdot I_D^m(t) \cdot \rho(t, C, h) \quad (\text{S9})$$

Here,  $I_D^w(t)$  and  $I_D^m(t)$  are the fluorescence intensity decays of Lz-A488 free in solution and membrane-bound to the lipid vesicles, respectively (described by a sum of exponentials (eqn (S5)) and  $\rho(t, C, h)$  is the FRET contribution to the donor decay. In case that each donor fluorophore, restricted to a single plane, senses only uniformly distributed acceptors located in the same bilayer at a transverse distance  $h$  (i.e., donors bound to proteins adsorbed on a lipid bilayer without any protein-mediated vesicle aggregation (single bilayer geometry (Fig. 1A)), the energy transfer term is given by:<sup>4,5</sup>

$$\rho(t, C, h) = \exp\left(-\frac{2C}{\Gamma(2/3)b} \int_0^1 \frac{1 - \exp(-tb^3 \alpha^6)}{\alpha^3} d\alpha\right) \quad (\text{S10})$$

where

$$C = \Gamma(2/3) \cdot n \cdot \pi \cdot R_0^2 \cdot \left(\langle \tau \rangle_2^{D,m}\right)^{-1/3} \quad (\text{S11})$$

and

$$b = (R_0/h)^2 \cdot (\langle\tau\rangle_2^{D,m})^{-1/3} \quad (\text{S12})$$

In these equations,  $\Gamma$  is the complete gamma function,  $R_0$  is the Förster radius ( $R_0 = 4.9$  nm for the Lz-A488/Rh-PE pair<sup>7</sup>) and  $\langle\tau\rangle_2^{D,m}$  is the intensity-weighted average of the membrane-bound donor lifetime in the absence of acceptor.<sup>6</sup> The acceptor surface density,  $n$  ( $n = (\text{acceptor:lipid mole ratio})/(\text{area per lipid molecule})$ ), was calculated for the system under study assuming a cross-sectional area of  $0.65 \text{ nm}^2$  for the phospholipids.<sup>9</sup> When the protein is able to cross-bridge the lipid vesicles, there are now two acceptor planes available for FRET (multilayer geometry (Fig. 1A)). Under the simplifying assumption that the protein-bound donor has a symmetrical position between the two leaflets, eqn (S10) is still valid but the numerical value of the surface concentration of acceptors should be doubled to take this new geometry into account.<sup>7</sup> In each case, only FRET between Lz-A488 and the nearest plane of acceptors is considered because according to the expected bilayer width of  $\sim 3.8 \text{ nm}$ <sup>7</sup>, FRET to further acceptor planes is negligible.

To retrieve important topological information from the system, a global analysis of the time-resolved fluorescence data was performed. Briefly, for each protein concentration, three experimental intensity fluorescence decays were analyzed simultaneously ( $I_D^W(t)$ ,  $I_D(t)$  and  $I_{DA}(t)$ , respectively). In order to decrease the number of freely optimizing fitting parameters, for each set of experimental decays obtained with a different Lz-A488 concentration,  $x_D^W$  was calculated independently according to the cooperative partition model described earlier<sup>8</sup> and held fixed in the global analysis. The pre-exponential ratios ( $a_2/a_1$  and  $a_3/a_1$ ) and the 3 lifetime components describing  $I_D^W(t)$  and  $I_D^m(t)$  (eqn (S5)) were either fixed or linked between the 3 experimental fluorescence decays being analyzed in each set, respectively. Therefore, the only free fitting parameters remaining were  $a_1$  for  $I_D^W(t)$  and  $I_D^m(t)$  each, the acceptor numerical

density ( $C$ ) and the donor-acceptor transverse interplanar distance ( $h$ ). Due to the strong correlation between these last two parameters, for each fixed value of  $h$ , a  $C$  value was obtained by minimizing the chi-square of the global fit,  $\chi_G^2$ . Finally, the theoretical expectation for the FRET efficiency due to membrane-bound donors only,  $E_{\text{FRET}}^m$ , was computed numerically from the fits obtained in the global analysis using:

$$E_{\text{FRET}}^m = 1 - \int_0^\infty I_{\text{DA}}^m(t) \cdot dt / \int_0^\infty I_{\text{D}}^m(t) \cdot dt \quad (\text{S13})$$

### **Infrared spectroscopy**

For the infrared measurements, approximately 25  $\mu\text{L}$  of sample in  $\text{D}_2\text{O}$  was placed between a pair of  $\text{CaF}_2$  windows separated by 56- $\mu\text{m}$  thick Teflon spacers in a liquid demountable cell (Harrick, Ossining, NY). Each spectrum was obtained by collecting 300 interferograms with a nominal resolution of 2  $\text{cm}^{-1}$  after transforming using triangular apodization. To obtain the average background spectra over the same time period of IR measurement, a sample accessory was used to shuttle the measurements between the sample and background spectra. The spectrometer was continuously purged with dry air at a dew point of  $-40$   $^\circ\text{C}$ , in order to remove atmospheric water vapor from the bands of interest. Protein secondary structure elements were quantified from curve-fitting analysis and band decomposition of the original amide I' band after background subtraction and spectral smoothing using GRAMS/32 or Spectra-Calc (Galactic Industries, Salem, MA), as previously described.<sup>10, 11</sup>

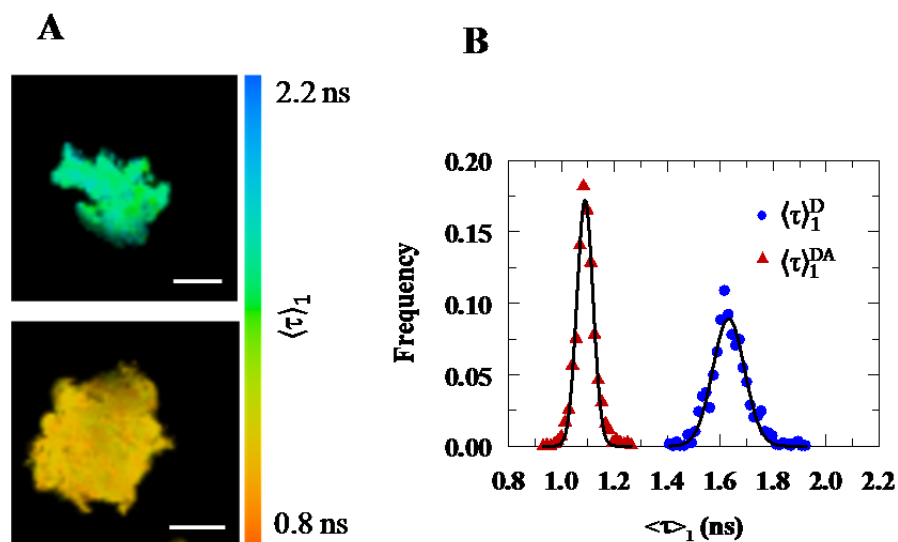


**Figure S1 - Representative images of FLIM-FRET measurements performed on irregularly-shaped aggregates.** (A) Mean fluorescence lifetime (FLIM) images of Lz-A488 in the absence (D, *top panel*) and presence of acceptors (DA, *bottom panel*). Scale bars correspond to 25  $\mu\text{m}$ . (B) Corresponding mean fluorescence lifetime histograms of D and DA in the mixed aggregates.

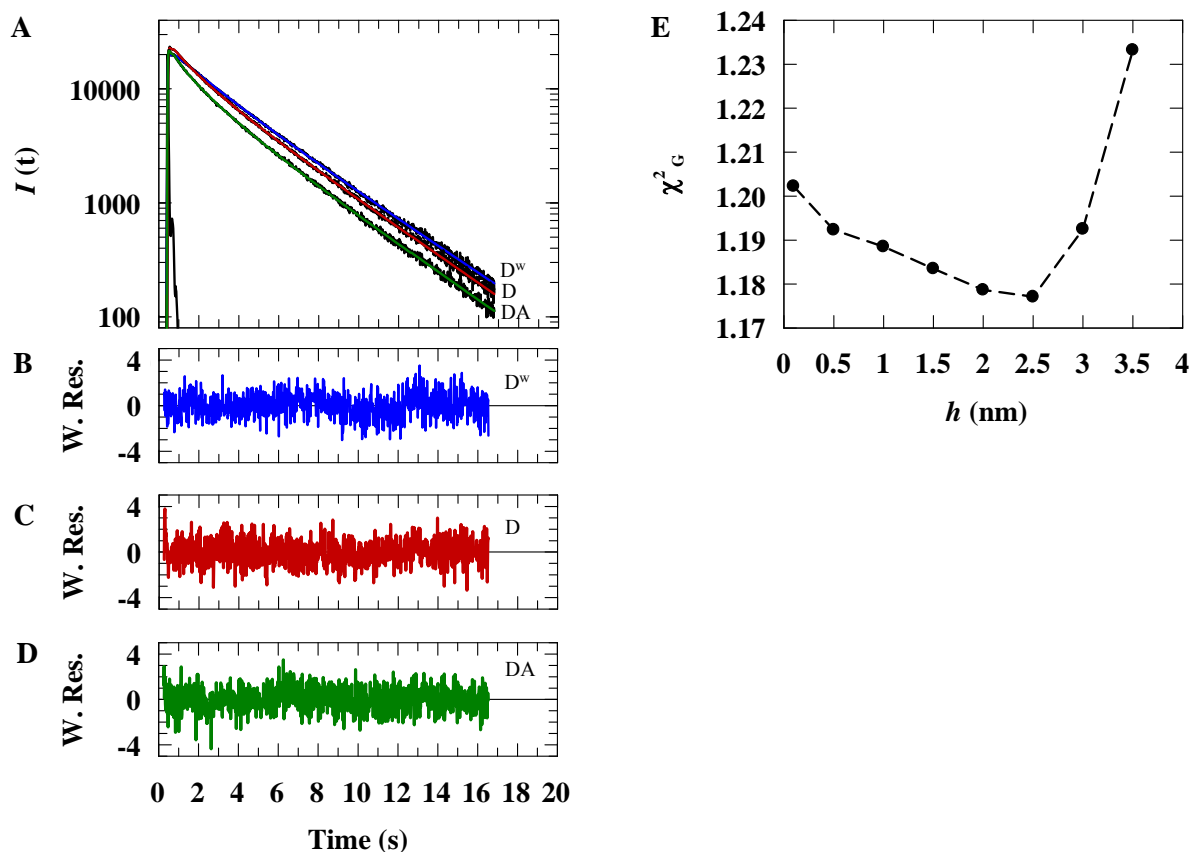


**Figure S2 – Global analysis of fluorescence decays obtained considering the presence of free isolated donors (unbound monomeric Lz-A488).** (A) Decay curves measured for 1  $\mu$ M Lz-A488 in aqueous solution ( $D^w$ ) and in the presence of 430  $\mu$ M POPC:POPS 80:20 LUVs, including or not the membrane-bound acceptor ( $DA$  and  $D$ , respectively). (B-D) Weighted residual plots obtained from the fits. (E) Global chi-square,  $\chi_G^2$ , obtained as a function of the donor-acceptor interplanar distance,  $h$ .

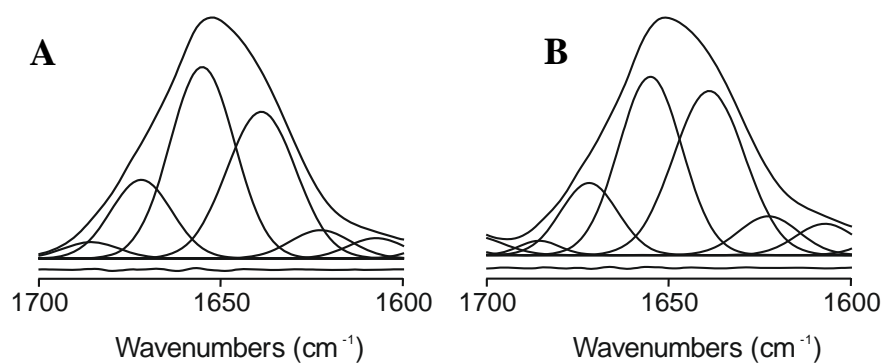


**Figure S3 – Infrared spectra in the range of the Amide I' band and fitted band components for (A) lysozyme in aqueous solution and (B) upon incubation with negatively-charged vesicles (POPC:POPG 80:20 LUVs) at a low *L/P* ratio.**

**Table S1** – Fitting parameters recovered from the fluorescence decay analysis of the brightest pixel of the FLIM-FRET images of the donor in the absence (D) and presence of membrane probes acceptor (DA) in the mixed lipid-protein fibers and aggregates.

<b>Sample</b>		<b><math>a_1</math></b> (%)	<b><math>\tau_1</math></b> (ns)	<b><math>a_2</math></b> (%)	<b><math>\tau_2</math></b> (ns)	<b><math>\langle\tau\rangle_1</math></b> (ns)	<b><math>E_{\text{FRET}}^{\text{FLIM}}</math></b>
Mixed Fibers ( $n=3$ )	D	$38 \pm 6$	$0.50 \pm 0.08$	$62 \pm 6$	$2.40 \pm 0.03$	$1.68 \pm 0.07$	$0.36$ $\pm 0.02$
	DA	$63 \pm 4$	$0.51 \pm 0.10$	$37 \pm 4$	$2.06 \pm 0.14$	$1.08 \pm 0.06$	
Aggregates ( $n=2$ )	D	$39 \pm 3$	$0.52 \pm 0.06$	$61 \pm 3$	$2.37 \pm 0.02$	$1.65 \pm 0.05$	$0.35$ $\pm 0.02$
	DA	$60 \pm 4$	$0.42 \pm 0.02$	$40 \pm 4$	$1.99 \pm 0.05$	$1.05 \pm 0.01$	

## References

1. FRAPAnalyser. <http://actinsim.uni.lu/eng/>. Accessed January 2013.
2. R. D. Phair, S. A. Gorski and T. Misteli, *Methods Enzymol.*, 2004, **375**, 393-414.
3. D. M. Soumpasis, *Biophys. J.*, 1983, **41**, 95-97.
4. L. Davenport, R. E. Dale, R. H. Bisby and R. B. Cundall, *Biochemistry*, 1985, **24**, 4097-4108.
5. C. Madeira, L. M. S. Loura, M. R. Aires-Barros, A. Fedorov and M. Prieto, *Biophys. J.*, 2003, **85**, 3106-3119.
6. L. M. S. Loura, A. Coutinho, A. Silva, A. Fedorov and M. Prieto, *J. Phys. Chem. B*, 2006, **110**, 8130-8141.
7. A. Coutinho, L. M. S. Loura, A. Fedorov and M. Prieto, *Biophys. J.*, 2008, **95**, 4726-4736.
8. A. M. Melo, J. C. Ricardo, A. Fedorov, M. Prieto and A. Coutinho, *J. Phys. Chem. B*, 2013, **117**, 2906-2917.
9. G. Lantzsch, H. Binder, H. Heerklotz, M. Wendling and G. Klose, *Biophys. Chem.*, 1996, **58**, 289-302.
10. A. Bernabeu, J. Guillen, A. J. Perez-Berna, M. R. Moreno and J. Villalain, *Biochim. Biophys. Acta-Biomembr.*, 2007, **1768**, 1659-1670.
11. M. Giudici, R. Pascual, L. de la Canal, K. Pfuller, U. Pfuller and J. Villalain, *Biophys. J.*, 2003, **85**, 971-981.